Acta Mechanica Slovaca **27 (4): 42 - 50,** December **2023**
https://doi.org/10.21496/ams.2023.039

Acta Mechanica Slovaca
ISSN 1335-2393
www.actamechanica.sk

Optimizing Earth-Air Heat Exchangers for Sustainable Summer Cooling and Winter Heating

Mohamed Amine Khorchef [1*], Mohamed Serier [2], Aboubakeur Benariba [3]

[1] GIDD Industrial Engineering and Sustainable Development Laboratory, Faculty of Engineering and Technology, University of Ahmed Zabana, Algeria
[2] LMPM, Department of Mechanical Engineering, University of Sidi Bel Abbes, BP 89 Cité Ben M'hidi 22000, Sidi Bel Abbes, Algeria
[3] Laboratory of Industrial Technologies, University of Tiaret, Tiaret, Algeria

Abstract: This study utilized a full factorial design with three factors at two levels each: thermal conductivity, pipe length, and air velocity. We aimed to identify optimal EAHE configurations for both summer cooling (maximum air temperature reduction) and winter heating (maximum temperature increase). Distinct optimal conditions emerged for each season. For summer cooling and winter heating, optimal configurations involved high thermal conductivity, moderate pipe length, and minimal air velocity. Statistical analysis revealed pipe length as the most influential factor on temperature in both seasons, explaining over 59% of the variability in winter and 49.43% in summer. Air velocity exerted a significant impact, while thermal conductivity had a smaller but still important influence. These findings showcase the effectiveness of full factorial design in unraveling complex interactions and pinpointing key parameters for EAHE optimization.

Keywords: Earth-air heat exchanger (EAHE), full factorial design, summer cooling, winter heating, Sustainable technologies.

1. Introduction

Energy consumption has surged dramatically over the past decade, primarily driven by rapid advancements in the residential, commercial, and industrial sectors. Buildings, for instance, consume over 40% of global energy and contribute to one-third of total greenhouse gas emissions [1]. Conventional heating and cooling systems pose significant environmental threats, including elevated CO2 emissions, global warming, intensified greenhouse effects, urban heat island phenomena, strained peak electrical demands, and compromised indoor air quality [2].

To achieve sustainable reductions in household energy consumption, consider implementing an earth-air heat exchanger (EAHE). This underground piping system harnesses ambient air for heating in winter and cooling in summer, minimizing energy consumption while maintaining indoor thermal comfort [3]. EAHE systems capitalize on the relatively stable soil temperature at depths between 1 and 6 m by employing underground pipes to transport indoor or outdoor air, facilitating effective thermal exchange [4–7].

Numerous studies have been conducted over the past two decades to develop analytical and numerical models for evaluating EAHE systems. A one-dimensional (1D) model was presented by De Paepe et al. [8] to investigate how an EAHE's design characteristics influence its thermal-hydraulic performance. Goswami et al. [9] developed a 1D time-dependent theoretical model to predict the efficiency of earth-to-air heat exchangers. Isotropic soil properties were assumed. Good agreement was found when comparing theoretical predictions with experimental observations. Fazlikhani et

*** Corresponding author:** Mohamed Amine Khorchef, ***E-mail address:*** *khorchef.mohamed@univ-relizane.dz*

al. [10] formulated a 1D steady-state model to assess EAHE performance, considering soil temperature variations but not thermal conductivity. Their model achieved a maximum relative difference of 1.7°C from experimental measurements. The findings demonstrated that as EAHE length increases, so does its efficiency.

Based on a two-dimensional (2D) numerical transient technique, Badescu [11] created a simple and accurate model of an EAHE that enabled the calculation of soil temperature at various depths and at the surface. To predict the thermal performance of earth-air-pipe heat exchanger systems, Bansal et al. [12, 13] developed a validated transient and implicit computational fluid dynamics (CFD) model within the FLUENT simulation tool. Excellent agreement was observed between simulated and experimental outcomes when the model was tested using experimental data from an Ajmer-based setup in Western India. Rosà et al. [14] simulated an EAHE's transient behavior using ANSYS-CFX® for heating and cooling. Results indicated that, for a fixed pipe diameter and spacing, increased airflow velocity reduced thermal performance, particularly during cooling (higher outlet air temperatures).

Design of experiments (DoE) efficiently plans experiments to extract meaningful information. It utilizes a minimal number of experiments, systematically varying multiple parameters simultaneously to gather sufficient data. This data then informs the development of a mathematical model for the studied process [15]. Response surface approach (RSM) is a powerful statistical tool for creating and refining product and process designs. It is a subclass of DoE methods [16] that has been employed by several researchers [17–19]. CFD technology was used to simulate all the necessary tests in order to construct the RSM model since it is significantly less expensive than conducting field experiments.

Statistical analysis plays a crucial role in scientific inquiry, enabling researchers to collect, interpret, and draw meaningful conclusions from data. The advancements in this field have significantly enhanced our ability to predict material behavior. For instance, [20] employed both Weibull and ANOVA analyses to investigate the B-basis values of CFRP composites, highlighting the suitability of the Weibull distribution and the limitations of ANOVA in specific cases. Similarly, [21] developed a multi-linear regression model to predict debonding loads in composites and concrete, demonstrating superior accuracy compared to alternative approaches. Furthermore, [22] combined ARIMA, ARTFIMA, and SVM models to achieve superior performance in greenhouse climate forecasting, showcasing the effectiveness of hybrid models. Finally, [23] introduced a novel correlation-based algorithm optimized with Shannon entropy for damage identification in aluminum plates, exemplifying the potential of advanced statistical approaches for material characterization.

This study seeks to develop innovative mathematical models using a unique approach that differs from previous research, specifically employing a full factorial design. The primary objective is to estimate the cooling and heating efficiency of EAHE within buildings during both the summer and winter seasons. The specific goals encompass: first, the development and validation of two mathematical models based on experimental data to predict the air temperature difference between the inlet and outlet; and second, the evaluation of the influence of the parameters under investigation using ANOVA. Third, the ultimate aim is to identify optimal parameter values that can substantially enhance the cooling and heating performance of EAHE systems.

2. Experimental

Figure 1 illustrates the deployment of an EAHE system featuring two horizontal cylindrical pipes with a 0.15m inner diameter and a buried length of 23.42m. Comprising a blend of PVC and mild steel materials, these pipes were buried at a depth of 2.7 m in level ground with dry soil. A 1 HP single-phase motorized blower operates at 2800 RPM and sustains an airflow rate of 0.033 m3/s through a vertical pipe connected to the subsurface pipe. The inlet and outlet temperatures of the subsurface pipe were denoted as Tinlet and Texit, respectively. A thermocouple at location (L = 10.03 m), identified as T1, measured the air temperature within the pipe. Valves allowed the adjustment of airflow through each pipe. Inlet temperatures and experimental data for both the summer and winter seasons were sourced from [12, 13].

3. Experimental design

To comprehensively evaluate the systematic

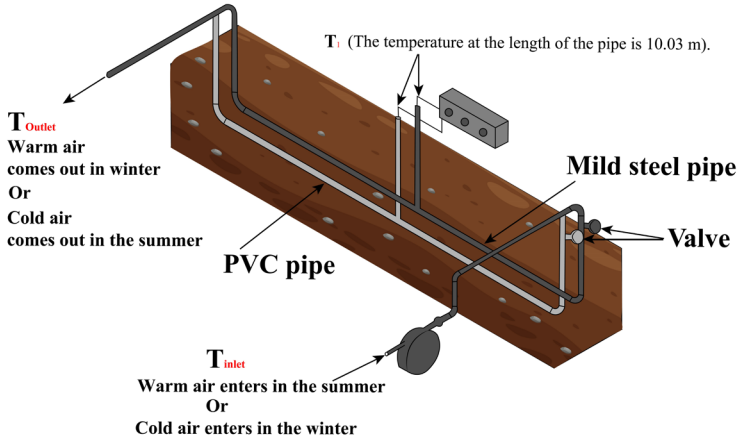

Figure 1: Illustrator image of the air-ground exchanger.

variations in response across different measurement conditions, a full factorial design with two levels (2k) was employed. This design enabled the simultaneous investigation of all potential interactions among the k = 3 independent variables, preventing any confounding effects that might arise from examining factors in isolation [24]. Equation (1) depicts the first-order polynomial model [25].

$$y = \beta_0 + \sum_{j=1}^{k} \beta_i X_j + \sum\sum_{i<j} \beta_{ij} X_i X_j + \varepsilon \qquad (1)$$

In the first-order polynomial model, β0 represents the mean score, βj denotes the linear factors, and βij represents the interaction factors. The letters Xj represent the model's factors, while factor combinations such as XiXj represent interactions between the various components.

This study delved into the influence of three key factors: pipe conductivity, which was varied between PVC 0.16 W/m.k and mild steel 54 W/m.k named (X1), pipe length (X2), and air velocity (X3), on the temperature response of the EAHE system. Temperature was considered as the dependent variable (response). Table 1 presents the three parameters and their respective levels employed in the experiment. Factor levels were denoted by the numbers -1 (low) and 1 (high). The results were subsequently analyzed with 95% confidence intervals.

3.1 Estimation of the sum of squares:

The initial stages of analyzing experimental design involve crucial computations to determine

Table 1: Experimental ranges and levels of independent variables.

Coded variable (Xi)	*Description*	*units*	*Experimental field*	
			Min. value (- 1)	*Max.value (+1)*
X_1	Pipe conductivity	(W/m.k)	0.16	54
X_2	Pipe length	(m)	10.0371	23.42
X_3	Air velocity	(m/s)	2	5

the effects of different factors and assess their statistical significance [26]. The effect of each factor on the response variable must be estimated. As shown in Equation (2), this estimation can be done for individual factors.

$$Effect = \frac{\sum_{i=1}^{n} y_i(+1) - \sum_{i=1}^{n} y_i(-1)}{n/2} \qquad (2)$$

Where n is the number of experimental points at each level and y is the corresponding response for each point.

The sum of squares of each factor and interaction is calculated analytically using Equation (3).

$$SS = \frac{N}{4}\left(Effect^2\right) \qquad (3)$$

Where N is the number of runs.

3.2 Regression and graphical analysis:

Regression analysis is employed to establish the mathematical relationship between independent factors and the response variable. The response is predicted using various combinations of process

parameters at their highest coefficient values [27]. STATISTICA software (Stat Soft, Inc., USA) version 10 was employed for data processing and analysis. STATISTICA is a comprehensive software package offering capabilities for statistical analysis, data mining, data visualization, and predictive modeling. Its diverse suite of tools caters to the needs of researchers, statisticians, and data analysts, facilitating thorough data exploration and insightful analysis. Graphical tools, including normal probability plots of residuals and contour plots, were utilized to analyze the factorial design and assess the adequacy of the fitted model.

3.3 Percentage contribution:

The percentage contribution of each parameter in a full factorial design quantifies the extent to which each factor influences the overall variability in the response variable. It is calculated as follows:

$$Percentage\ contribution\ of\ factor_i = \left(\frac{SS_i}{Total_{ss}}\right)\cdot 100 \quad (4)$$

Where:

- *SSi is the sum of squares for factor i.*
- *Total SS is the total sum of squares.*

4. Results and Discussion

4.1 Experimental results:

Table 2 presents the design matrix for EAHE system, including real variables and experimental responses. Real variables represent the actual values for pipe conductivity, pipe length, and air velocity. The responses, represented as temperatures (Y_1 and Y_2), correspond to the outcomes observed during both the summer and winter seasons.

Table 2: Experimental data.

Experiment	*X_1: Pipe conductivity (W/m.k)*	*X_2: Length of Pipe (m)*	*X_3: Air velocity (m/s)*	*Temperature (k)*	
				Y_1	Y_2
1	0.16	10.037	2	24	35
2	54	10.037	2	24.3	33.6
3	0.16	23.42	2	25.1	33.1
4	54	23.42	2	25.4	31
5	0.16	10.037	5	22.9	37
6	54	10.037	5	23.3	36.5
7	0.16	23.42	5	24.2	34.2
8	54	23.42	5	24.7	33.7

4.2 Optimization by full factorial design:

Regression analysis yielded a predictive model for EAHE system temperature based on the experimental data collected. The resulting first-order polynomial equation (Equations 5 and 6) reveals the intricate relationship between coded factors (pipe conductivity, pipe length, and air velocity, denoted by X_1, X_2, and X_3) and response variables (Y_1 for winter and Y_2 for summer). This model empowers researchers to make predictions for specific factor levels, paving the way for optimized EAHE system design and operation.

Figures 2a and 2b present normal probability plots (NPPs) to assess the normality of the residuals and the differences between observed and predicted responses in our models. Verifying residual normality is critical for ensuring the validity of statistical inferences drawn from the model. The horizontal axis in both NPPs represents predicted values, while the vertical axis represents observed values. The close adherence of data points to the straight reference line in both figures suggests that the residuals follow a normal distribution, supporting the validity of our models and the reliability of the conclusions drawn from them. This adherence shows that the models correctly show the underlying relationships in the data without big departures from normality. This makes our statistical conclusions more reliable.

Table 3 presents the results of the analysis of variance (ANOVA) performed for the winter season. The model F-value, reaching an impressive 671.67, unequivocally highlights the overall significance of the model. The corresponding P-value of 0.0295 implies a negligible 2.95% probability of obtaining such a substantial F-value by chance, firmly establishing the model's statistical significance.

Delving into individual model terms reveals that P-values below 0.05 indicate significant effects. Notably, the terms (X_1) pipe conductivity, (X_2) pipe length, and (X_3) air velocity are all statistically significant, as evidenced by their respective P-values of 0.042379*, 0.012990*, and 0.017202*. It is noteworthy that none of the interaction terms (X1X2, X1X3, X2X3) achieve statistical significance, as their P-values all surpass 0.05. The error row represents unexplained variability with a mean

$$Y_1 = 24.2375 + 0.1875X_1 + 0.6125X_2 - 0.4625X_3 + 0.0125X_1X_2 + 0.0375X_1X_3 + 0.0625X_2X_3 \quad (5)$$

$$Y_2 = 34.2625 - 0.5625X_1 - 1.2625X_2 + 1.0875X_3 - 0.0875X_1X_2 + 0.3125X_1X_3 - 0.1375X_2X_3 \quad (6)$$

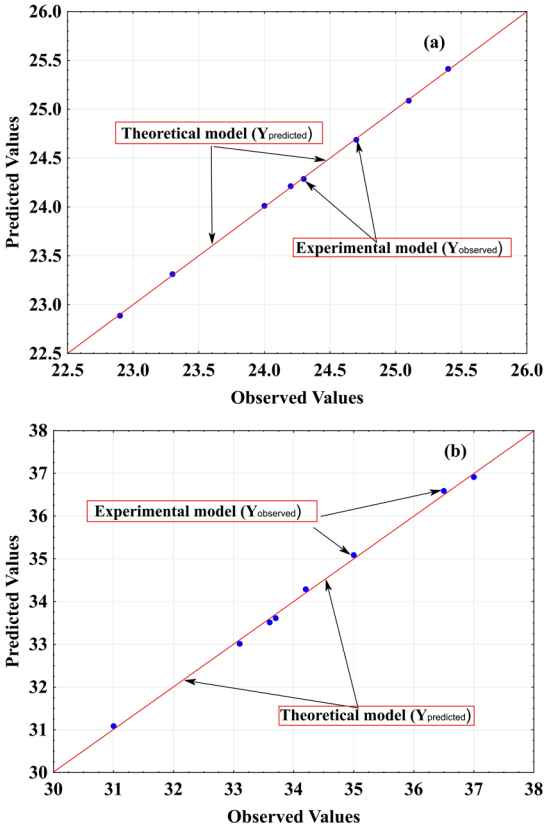

Figure 2: Normal probability plot of residuals. (a) Represents the results of the winter season. (b) Represents the results of the summer season.

square (MS) of 0.00125. Total SS (sum of squares) serves as an overall measure of variability in the response variable.

Table 4 presents the ANOVA results for the summer season. The model F-value of 70.03 indicates overall significance, with a 9.12% probability of obtaining such a large F-value due to random fluctuations. Among individual model terms, only factor X_2 (pipe length) exhibits statistical significance, as evidenced by a P-value of 0.044052*. None of the interaction terms (X_1X_2, X_1X_3, and X_2X_3) demonstrate statistical significance, as their P-values surpass 0.05. The error row represents unexplained variability with a mean square (MS) of 0.06125.

Figure 3 provides temperature contour maps inside the EAHE at constant airflow (5m/s). The graphic demonstrates the impact of pipe length (8–24m) and conductivity (0–60W/m.K.) on temperature distribution. Higher temperatures (red) concentrate towards the outlet and with increasing conductivity (use mild steel pipe 54W/m.K.). Extending length to 21–24m further enhances heat extraction, indicating an ideal equilibrium for maximum EAHE performance.

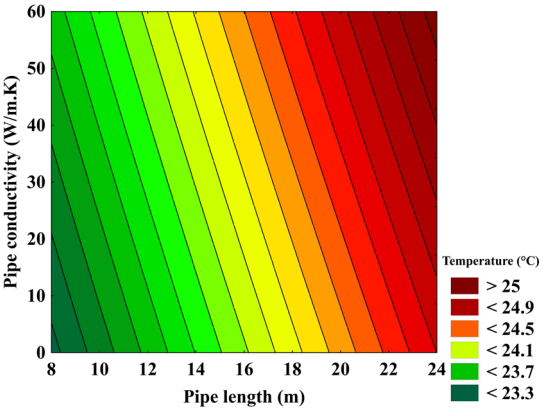

Figure 3: illustrates the influence of pipe length and pipe conductivity on the temperature distribution for winter seasons.

Table 3: Results of ANOVA for winter.

	Effect	*SS*	*Df*	*MS*	*F-ratio*	*P-value*
Model		5.04	6	0.8396	671.67	0.0295*
(X_1) pipe conductivity	0.375	0.28125	1	0.28125	225	0.042379*
(X_2) pipe length	1.225	3.00125	1	3.00125	2401	0.012990*
(X_3) air velocity	-0.925	1.71125	1	1.71125	1369	0.017202*
X_1X_2	0.025	0.00125	1	0.01125	1	0.5
X_1X_3	0.075	0.01125	1	0.01125	9	0.2048
X_2X_3	0.125	0.03125	1	0.03125	25	0.1256
Error		0.00125	1	0.00125		
Total SS		5.03875	7			

Table 4: Results of ANOVA for summer.

	Effect	*SS*	*Df*	*MS*	*F-ratio*	*P-value*
Model		25.74	6	4.29	70.03	0.0912
(X_1) pipe conductivity	-1.125	2.53125	1	2.53125	41.3265	0.098242
(X_2) pipe length	-2.525	12.75125	1	12.75125	208.1837	0.044052*
(X_3) air velocity	2.175	9.46125	1	9.46125	154.4694	0.051112
X_1X_2	-0.175	0.06125	1	0.06125	1	0.5
X_1X_3	0.625	0.78125	1	0.78125	12.7551	0.173803
X_2X_3	0.275	0.15125	1	0.15125	2.4694	0.360791
Error		0.06125	1	0.06125		
Total SS		25.79875	7			

Figure 4 depicts the temperature distribution as a function of pipe length and air velocity. Pipe length (8–24m) is displayed on the horizontal axis, and air velocity (1.5–5.5m/s) on the vertical axis. The colormap indicates the EAHE temperature, with green colors denoting temperatures below 22.5°C and red hues surpassing 25°C. Thermal conductivity remained constant at 0.16W/m.K.; significantly, increased air velocity leads to decreased air temperature. This may be due to the decreased air residence time in the pipes, which reduces heat exchange with the ground and decreases the outgoing air temperature.

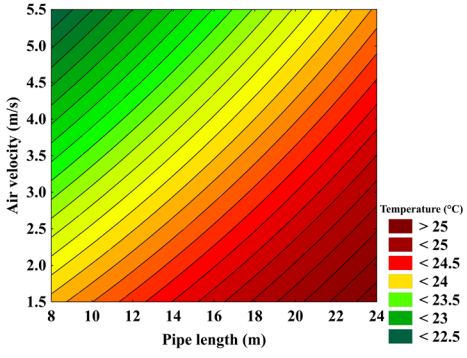

Figure 4: illustrates the influence of pipe length and air velocity on the temperature distribution for winter seasons.

Figures 3 and 4 represent winter season results; maximizing temperature is crucial for heating applications. To achieve temperatures exceeding 24.5 degrees Celsius, the study suggests air velocity below 2.5m/s and a pipe length exceeding 20m, up to a maximum of 22m. increasing the pipe length beyond this point becomes progressively impractical. And use a pipe with high thermal conductivity.

Figure 5 illustrates the temperature distribution in response to pipe length and air velocity. The x-axis shows pipe length, ranging from 8 to 24m, while the y-axis depicts air velocity, which varies from 1 to 5.5 m/s. A colormap delineates the temperature range (32.75°C–<37°C), where colder shades of green represent lower temperatures, while warmer red colors signify higher values. The maximum temperature is seen at the pipe at 8m, corresponding to the hottest air. As the air crosses the pipe, it undergoes cooling owing to heat exchange with the nearby earth. This cooling impact lessens with increased air velocity, suggesting decreased time for heat exchange with the earth.

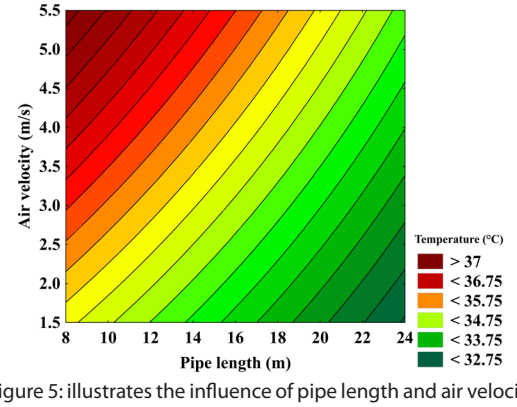

Figure 5: illustrates the influence of pipe length and air velocity on the temperature distribution for summer seasons.

Figure 6 depicts the temperature distribution considering varying pipe lengths and conductivities. The abscissa delineates the pipe's length, extending from 8 to 24m, while the ordinate illustrates the thermal conductivity of the pipe, swinging between 0 and 60W/m.K. The color gradient represents the temperature within the EAHE system: shades of green correlate to colder temperatures (<32.25°C),

and red colors imply higher temperatures (>36°C). As predicted, the research suggests that the most muted temperatures materialize in the top right quadrant of the contour plot, characterized by extended pipes and heightened thermal conductivity. This effect is attributable to the greater surface area of longer pipes, permitting higher heat exchange with the neighboring earth. Additionally, materials with increased conductivity display greater heat transfer efficiency. In contrast, the highest increased temperatures are centered in the bottom left quadrant, characterized by shorter pipe lengths and decreased thermal conductivity. For best summertime circumstances, the study suggests keeping a thermal conductivity of 54W/m.k., sticking to pipe lengths between 20 and 22m, and confining the airflow velocity ratio to a maximum threshold of 2.5m/s.

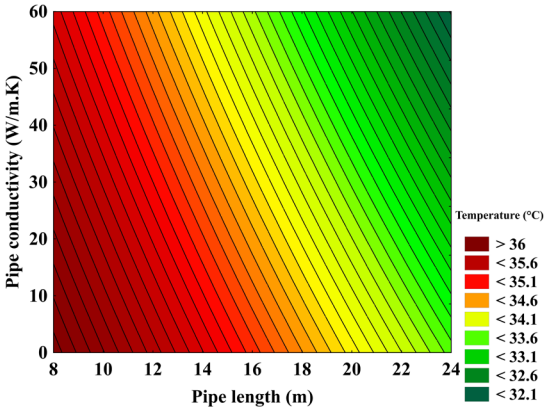

Figure 6: illustrates the influence of pipe length and pipe conductivity on the temperature distribution for summer seasons.

4.3 Percentage contribution of each parameter:

Figure 7 delineates the proportionate contributions of each components to the total temperature fluctuation over winter and summer, derived by Equation (4). Pipe length significantly comes up as the key factor in both seasonal studies, contributing 59.56% and 49.43% of the variability for winter and summer, respectively. Air velocity follows as the second important element, accounting for 33.96% in winter and 36.67% in summer. Conversely, thermal conductivity has a considerably weaker influence, accounting for a moderate 5.58% in winter and 9.81% in summer of the measured range.

5. Conclusions

This study employed a full factorial design technique to optimize the summer air temperature decrease and winter air temperature increase in an earth-air heat exchanger (EAHE) system for both heating and cooling applications. Three operational parameters were investigated at two levels each, yielding a total of eight experimental runs. The key findings and observations of the study are as follows:

– *A first-order polynomial model accurately predicts EAHE system temperatures based on coded operational parameters (pipe conductivity, length, and air velocity). This empowers researchers and engineers to optimize system design and operation for specific seasonal requirements, contributing to more efficient and sustainable heating and cooling solutions.*

– *Model validity confirmed: Statistical analysis and normal probability plots validate the model's reliability, ensuring accurate data representation and reliable predictions.*

– *Significant factors identified: pipe length emerges as the dominant factor influencing temperature in both winter and summer, followed by air velocity. Thermal conductivity plays a smaller role, but its*

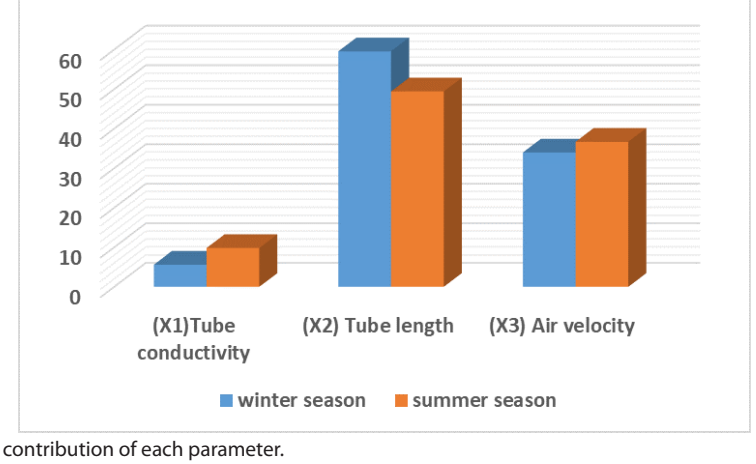

Figure 7: Percentage contribution of each parameter.

optimization can still enhance system performance.

– Seasonal recommendations: distinct optimal operating conditions are identified for winter and summer. Maximizing and reducing temperature in winter and summer requires mild steel pipes, longer lengths (21–24m), and limiting air velocity (2.5m/s).

– Employing a full factorial design in this (EAHE) study proved instrumental, yielding a rich dataset of immense value. This robust experimental method lays a solid foundation for further research and in-depth analysis in this field.

– Future research directions: expanding the model to include additional influencing factors, validating it across diverse soil types and climates, and exploring its potential for real-time EAHE control are promising avenues for future research, further advancing sustainable heating and cooling technologies.

Abbreviations

EAHE	Earth-Air Heat Exchanger
CO2	Carbon Dioxide
1D	One-dimensional
2D	Two-Dimensional
CFD	Computational Fluid Dynamics
ANSYS-CFX	ANSYS-Computational Fluid Dynamics
DOE	Design of Experiments
RSM	Response Surface Methodology
ANOVA	Analysis of Variance
ARIMA	Auto Regressive Integrated Moving Average
ARTFIMA	Auto Regressive Fractionally Integrated Moving Average
SVM	Support Vector Machine
CFRP	Carbon Fiber Reinforced Polymer
PVC	Polyvinyl Chloride
HP	Horsepower
RPM	Revolutions Per Minute
MSresidual	Mean square of the residuals
SS	Sum of squares
NPP	Normal probability plots
MS	Mean Square

References

[1] G. Mihalakakou, M. Souliotis, M. Papadaki, G. Halkos, J.,Paravantis, S. Makridis, , S. Papaefthimiou, (2022). Applications of earth-to-air heat exchangers: a holistic review. Renewable and Sustainable Energy Reviews, 155, 111921.

[2] S. Karytsas, H. Theodoropoulou, (2014). Public awareness and willingness to adopt ground source heat pumps for domestic heating and cooling. Renewable and Sustainable Energy Reviews, 34, 49-57.

[3] K. Anshu, P. Kumar, B. Pradhan, (2023). Numerical simulation of stand-alone photovoltaic integrated with earth to air heat exchanger for space heating/cooling of a residential building. Renewable Energy, 203, 763-778.

[4] A. Zajch, W. A. Gough, (2021). Seasonal sensitivity to atmospheric and ground surface temperature changes of an open earth-air heat exchanger in Canadian climates. Geothermics, 89, 101914.

[5] R. Singh, R. L. Sawhney, I. J. Lazarus, V. V. N. Kishore, (2018). Recent advancements in earth air tunnel heat exchanger (EATHE) system for indoor thermal comfort application: A review. Renewable and Sustainable Energy Reviews, 82, 2162-2185.

[6] S. Mongkon, S. Thepa, P. Namprakai, N. Pratinthong, (2013). Cooling performance and condensation evaluation of horizontal earth tube system for the tropical greenhouse. Energy and Buildings, 66, 104-111.

[7] N. Bordoloi, A. Sharma, H., Nautiyal, V. Goel, (2018). An intense review on the latest advancements of Earth Air Heat Exchangers. Renewable and Sustainable Energy Reviews, 89, 261-280.

[8] M. De Paepe, A. Janssens, (2003). Thermo-hydraulic design of earth-air heat exchangers. Energy and buildings, 35(4), 389-397.

[9] D. Y. Goswami, A. S. Dhaliwal, (1985). Heat transfer analysis in environmental control using an underground air tunnel. ASME. J. Sol. Energy Eng, 107(2), 141–145.

[10] F. Fazlikhani, H. Goudarzi, E. Solgi, (2017). Numerical analysis of the efficiency of earth to air heat exchange systems in cold and hot-arid climates. Energy conversion and management, 148, 78-89.

[11] V. Badescu, (2007). Simple and accurate model for the ground heat exchanger of a passive house. Renewable energy, 32(5), 845-855.

[12] V. Bansal, R. Misra, G. D. Agrawal, J. Mathur, (2009). Performance analysis of earth–pipe–air heat exchanger for winter heating. Energy and Buildings, 41(11), 1151-1154.

[13] V. Bansal, R. Misra, G. D. Agrawal, J. Mathur, (2010). Performance analysis of earth–pipe–air heat exchanger for summer cooling. Energy and buildings, 42(5), 645-648.

[14] N. Rosa, N. Soares, J. J. Costa, P. Santos, H. Gervásio, (2020). Assessment of an earth-air heat exchanger (EAHE) system for residential buildings in warm-summer Mediterranean climate. Sustainable Energy Technologies and Assessments, 38, 100649.

[15] W. G. Whitford, M. Lundgren, A. Fairbank, (2018). Cell culture media in bioprocessing. G. Jagschies, E. Lindskog, K. Łącki, P. Galliher, In Biopharmaceutical Processing, Elsevier, 147-162.

[16] A. Jahan, K. L. Edwards, M. Bahraminasab, (2016). 6-Multiple objective decision-making for material and geometry design. Multi-criteria decision analysis for supporting the selection of engineering materials in product design. Elsevier, 127-146.

[17] M. Kaushal, P. Dhiman, S. Singh, H. Patel, (2015). Finite volume and response surface methodology based performance prediction and optimization of a hybrid earth to air tunnel heat exchanger. Energy and Buildings, 104, 25-35.

[18] S. Ali, N. Muhammad, A. Amin, M. Sohaib, A. Basit, T. Ahmad, (2019). Parametric optimization of earth to air heat exchanger using response surface method. Sustainability, 11(11), 3186.

[19] X. Wang, B. S. Bjerg, G. Zhang, (2018). Design-oriented modelling on cooling performance of the earth-air heat exchanger for livestock housing. Computers and Electronics in Agriculture, 152, 51-58.

[20] D. Tamaza, D. Widagdo, M. Kusni, B.K. Hadi, (2020). Statistical analysis of CFRP mechanical properties using B-basis based on weibull and ANOVA distribution analysis. In IOP Conference Series: Materials Science and Engineering, 012078.

[21] S. Kebdani, (2021). Statistical analysis of debonding fiber-reinforced polymer plate and sheet. Acta Technica Napocensis-Series: Applied Mathematics, Mechanics, and Engineering. 64(4), 615-624.

[22] M. Seba, D. Seba, A. Berkani, B. Mekhloufi, (2023). Hybrid approach for prediction of temperature and moisture in greenhouses using Arima, Artfima and Svm methods. Applied ecology and environmental research. 21(6), 5737-5751.

[23] D. Wang, L. Ye, Z. Su, Y. Lu, F. Li, and G. Meng, (2010). Probabilistic damage identification based on correlation analysis using guided wave signals in aluminum plates. Structural Health Monitoring. 9(2), 133-144.

[24] R. F. Galbraith, R. G. Roberts, (2012). Statistical aspects of equivalent dose and error calculation and display in OSL dating: An overview and some recommendations. Quaternary Geochronology, 11, 1-27.

[25] D. C. Montgomery, (2017). Design and analysis of experiments. John wiley & sons.

[26] M.J. Anderson, P.J. Whitcomb, (2017). DOE simplified: practical tools for effective experimentation. CRC press.

[27] J, Antony, (2003). Design of Experiments for Engineers and Scientists, Oxford: Elsevier Butterworth-Heinemann, United Kingdom.